

PLANETARY NEBULAE AS STANDARD CANDLES. XI. APPLICATION TO SPIRAL GALAXIES

John J. Feldmeier and Robin Ciardullo^{1,2}

Department of Astronomy and Astrophysics, Penn State University
525 Davey Lab, University Park, Pennsylvania 16802

and

George H. Jacoby

Kitt Peak National Observatory, National Optical Astronomy Observatories
P.O. Box 26732, Tucson, AZ 85726

¹ Visiting Astronomer, Kitt Peak National Optical Astronomy, National Optical Astronomical Observatories, operated by the Association of Universities for Research in Astronomy, Inc., under cooperative agreement with the National Science Foundation.

²NSF Young Investigator

Abstract

We report the results of an [O III] $\lambda 5007$ survey for planetary nebulae (PN) in three spiral galaxies: M101 (NGC 5457), M51 (NGC 5194/5195) and M96 (NGC 3368). By comparing on-band/off-band [O III] $\lambda 5007$ images with images taken in $H\alpha$ and broadband R , we identify 65, 64 and 74 PN candidates in each galaxy, respectively. From these data, an adopted M31 distance of 770 kpc, and the empirical planetary nebula luminosity function (PNLF), we derive distances to M101, M51, and M96 of 7.7 ± 0.5 , 8.4 ± 0.6 , and 9.6 ± 0.6 Mpc. These observations demonstrate that the PNLF technique can be successfully applied to late-type galaxies, and provide an important overlap between the Population I and Population II distance scales. We also discuss some special problems associated with using the PNLF in spiral galaxies, including the effects of dust and the possible presence of [O III] bright supernova remnants.

Subject Headings: galaxies: distances and redshifts — distance scale — galaxies: individual (M101, NGC 5457, M51, NGC 5194, M96, NGC 3368) — planetary nebulae: general — supernova remnants

1. Introduction

The planetary nebula luminosity function (PNLF) is a distance indicator for galaxies potentially as far away as ≈ 25 Mpc. It has proved to be remarkably successful for many galaxies, including galaxies in the Virgo cluster (Jacoby, Ciardullo, & Ford 1990a), the Fornax cluster (McMillan, Ciardullo, & Jacoby 1993), and the Magellanic Clouds (Jacoby, Walker, & Ciardullo 1990b). For a complete review, see Jacoby *et al.* (1992).

The PNLF uses the observational result, supported by theory (Jacoby 1989; Han, Podsiadlowski, & Eggleton 1994; Méndez *et al.* 1993; Stanghellini 1995), that the luminosity function of planetary nebulae (PN), in the light of [O III] $\lambda 5007$, has the form

$$N(M) \propto e^{0.307M} [1 - e^{3(M^* - M)}] \quad (1)$$

(Ciardullo *et al.* 1989a). Assuming that this function is correct, we can compare the PNLF in a distant galaxy to a PNLF in a nearby galaxy whose distance is already known from some other method. The calibration for the PNLF is currently provided by M31, whose distance is well known from Cepheid variables (Freedman & Madore 1990). This calibration has been validated by checks in M81 (Jacoby *et al.* 1989), the LMC (Jacoby, Walker, & Ciardullo 1990b), and NGC 300 (Soffner *et al.* 1996).

Until now, the PNLF technique has been used primarily in elliptical and S0 galaxies, where the problems presented by internal extinction and interloping H II regions are minimal. However, since planetary nebulae are not associated with any one stellar population, PN measurements in spirals should be possible. Specifically, it should be possible to discriminate planetary nebulae from H II regions on the basis of their [O III]/ $H\alpha$ line ratio. Bright planetary nebulae are high excitation objects, hence $I(\lambda 5007)/I(H\alpha) > 1$; the opposite is true for H II regions.

There are a number of reasons to attempt to apply the PNLF technique to spiral galaxies. First, observing the PNLF in more luminous galaxies allows us to check for internal consistency of the method. Critics have proposed that the maximum magnitude of the PNLF, M^* , increases with the absolute magnitude of the galaxy (Bottinelli *et al.* 1991). Clearly, observing bright galaxies along with dimmer galaxies in a cluster would test this hypothesis. This has already been done in the Fornax cluster (McMillan, Ciardullo, & Jacoby 1993), and in the Virgo cluster (Jacoby, Ciardullo,

& Ford 1990a), but doing more high luminosity galaxies, such as bright spirals, would constrain the invariance of M^* even further.

Secondly, since the PNLF has been primarily used in old stellar populations, it is possible that M^* depends on population age. Han, Podsiadlowski, & Eggleton (1994), Méndez *et al.* (1993), Stanghellini (1995), and Soffner *et al.* (1996) have all proposed that M^* may be brighter in younger stellar populations. The way to test this hypothesis is to observe galaxies with ongoing star formation, such as late-type spirals.

Finally, the most important test of any distance method is its comparison with other methods. A fundamental weakness of the current extragalactic distance scale is the small amount of overlap and cross-checks between some of the techniques. In fact, there are actually two distinct distance scales: a Population II scale, defined by the planetary nebula luminosity function (PNLF), surface brightness fluctuations (SBF), the globular cluster luminosity function (GCLF), and the elliptical galaxy fundamental plane ($D_n-\sigma$) relations, and a Population I scale, involving Cepheid variables, supernovae, and the Tully-Fisher relation. Remarkably, there are only five galaxies common to both systems: M31, the Large Magellanic Cloud, NGC 5253, M81, and NGC 300. Despite all the checks and comparisons, the calibration of the Population II distance scale rests solely on these five galaxies. All other calibrations are indirect (*i.e.*, they use different galaxies within a common cluster), and are thus susceptible to systematic errors due to galaxy segregation.

The best method of linking the two distance scales is through the planetary nebula luminosity function. Unlike Cepheids, which are exclusively Population I objects, or the SBF method, which can only be applied in relatively red galaxies with smooth isophotal profiles, PNLF measurements can (in theory) be performed in any galaxy, as long as there are enough bright PN to populate the bright end of the luminosity function. Thus, the PNLF has the potential to be *both* a Population I and II distance indicator, assuming there are no systematic biases with galaxy type. The purpose of this paper is to test whether this is true.

2. Observations and Data Reduction

The observations were obtained on 1995 April 5-8, and 11 using the prime focus of the Kitt Peak 4-m telescope and the T2KB 2048 x 2048 Tektronix CCD, which has a pixel scale of $0''.47$ per pixel

and a field-of-view of $16' \times 16'$. We obtained exposures for three galaxies, M101 (NGC 5457), M51 (NGC 5194 and NGC 5195), and M96 (NGC 3368), through a 30 \AA wide [O III] $\lambda 5007$ filter centered on the galaxies' systemic velocities. Corresponding images were then taken through a 275 \AA wide off-band filter (central wavelength $\sim 5300 \text{ \AA}$), a 75 \AA wide $H\alpha$ filter, and a broadband R filter. The seeing throughout the observations was always better than $1''.2$. A log of these observations is given in Table 1. The data were bias-subtracted and flat-fielded at the telescope, using the IRAF reduction system.

Our survey technique was as described in previous papers (*e.g.*, Jacoby *et al.* 1989; Ciardullo, Jacoby, & Ford 1989b). We identified PN candidates by “blinking” the sum of the on-band [O III] images for each galaxy against a corresponding off-band sum. In order to discriminate planetary nebulae from other emission line sources, we used the following criteria: 1) PN candidates had to have a point-spread-function (PSF) consistent with that of a point source; 2) PN candidates had to be present on the [O III] $\lambda 5007$ image, but invisible on the off-band image; and 3) PN candidates had to be invisible in R and invisible in $H\alpha$. In addition, to further reduce the possibility of contamination from H II regions, we did not attempt to find planetary nebulae within the obvious star-forming regions of the galaxies (*i.e.*, the spiral arms); instead, we concentrated our search in the galactic halos and inter-arm regions.

By applying the above criteria, we severely reduced the possibility of an H II region accidentally being included in our list of planetary candidates. At a distance of $\sim 10 \text{ Mpc}$, one arcsecond is equivalent to $\sim 48 \text{ parsecs}$, thus we resolved the majority of H II regions out of our sample. Similarly, by requiring that PN candidates be invisible on the off-band and R -band frames, we excluded those emission-line regions that have bright, exciting OB-stars. Our most valuable condition, however, was the [O III] $\lambda 5007$ to $H\alpha$ emission line ratio. Unlike bright planetary nebulae, H II regions are usually low excitation objects with $I(\lambda 5007)/I(H\alpha) < 1$. However, to be considered a planetary nebula candidate, an object had to have an [O III] $\lambda 5007$ to $H\alpha$ ratio greater than 1.6. (For the faintest PN in the sample, $I(\lambda 5007)/I(H\alpha)$ had to be ~ 1.6 , which was the ratio of the detection limits of the two images; for brighter PN, the minimum line ratio was greater, since we required that all PN candidates be invisible in $H\alpha$.) In the Shaver *et al.* (1983) sample of Galactic H II regions, only 11% of the objects have an [O III] to $H\alpha$ ratio greater than 1.6, and only one out of

39 has $I(\lambda 5007)/I(H\alpha) > 3$. Conversely, the [O III] $\lambda 5007$ PNLFs defined in other galaxies (*e.g.*, M31: Ciardullo *et al.* 1989a; M81: Jacoby *et al.* 1989; NGC 891: Ciardullo, Jacoby, & Harris 1991; NGC 4565 and 4278: Jacoby, Ciardullo, & Harris 1996; M87: Ciardullo, Jacoby, & Feldmeier 1997) include only those objects with $I(\lambda 5007)/I(H\alpha) \gtrsim 2.0$. Thus, by excluding those objects that are $H\alpha$ bright, we removed most of the H II regions from the sample while leaving the bright end of the [O III] PNLF intact.

With all the above constraints, only compact, inter-arm H II regions that have high nebula excitation and faint central OB associations will have been mistaken for planetary nebulae. However, even these objects will not significantly affect our PNLF. Because our threshold $I(\lambda 5007)/I(H\alpha)$ ratio is more stringent for brighter objects, any H II regions that do make it into our sample will be faint in [O III] and fall below our photometric completeness limit (described below). We are therefore confident that essentially all the objects in our sample are, indeed planetary nebulae, and not H II regions. Furthermore, as we shall see below, the agreement between the observed shapes of the PNLF's, and the agreement between the PNLF and Cepheid distances provides a validity check on our H II region exclusion criteria. Had the PN sample been seriously contaminated by bright H II regions the PNLF fits to the empirical law would have been poor and our distances would have been systematically and unpredictably too small.

In total, we identified 65 candidate planetaries in M101, 64 in M51, and 74 in M96. Sample images of candidate planetary nebulae in the light of [O III] $\lambda 5007$, $H\alpha$, and offband [O III] are given in Figure 3 of Feldmeier, Ciardullo, & Jacoby (1996).

The PN candidates were measured photometrically using the IRAF version of DAOPHOT (Stetson 1987), and flux calibrated using Stone (1977) standard stars and the procedures outlined by Jacoby, Quigley, & Africano (1987). The resulting monochromatic fluxes were then converted to m_{5007} magnitudes using

$$m_{5007} = -2.5 \log F_{5007} - 13.74 \quad (2)$$

Astrometry was performed using the positions of stars in the *Hubble Space Telescope* Guide Star Catalog (GSC). In most cases, the GSC stars were saturated, requiring us to use a two-step process. First, we used digitized images of the Palomar Sky Survey to measure the positions of unsaturated

stars on our CCD frames relative to stars in the GSC catalog. We then found the positions of our PN candidates relative to these secondary standards. Based on the residuals of our fits, we estimate that these positions are accurate to $0''.68$ in M101, $0''.49$ in M51, and $0''.44$ in M96.

3. Fitting the PNLFs and Obtaining Distances

Before we can fit our observed luminosity functions to equation (1), we must estimate our photometric completeness level. Because our PN survey was conducted primarily in the low surface-brightness regions of each galaxy, our ability to detect PN was not a strong function of galactic position. Thus, we used the results of Jacoby *et al.* (1989) and Hui *et al.* (1993) to estimate our limiting magnitude for completeness as the place where the PNLF (which should be exponentially increasing) begins to turn down. To confirm this number, we randomly added artificial stars to our summed on-band images, and reblinked the frames to recover as many of the simulated objects as possible. As expected, the fraction of our recoveries was independent of PN magnitude down to about the completeness level, except in the spiral arms and innermost regions of the galaxies.

Unfortunately, due to the complex and variable backgrounds presented by our target galaxies, the detectability of each planetary is different, and this could possibly change the shape of the observed luminosity function. To deal with this problem, we created a statistical sub-sample of PN in each galaxy, for which the effects of the sky background were minimal. To form this sample, we began by noting the median sky background associated with each PN measurement. After excluding those few objects superposed on bright regions of the galaxy, we picked the worst (most uncertain) background remaining in the sample, and computed the signal-to-noise each PN would have, if it were projected on that background. Only those objects which would have been detected with a signal-to-noise greater than 10 (cf. Ciardullo *et al.* 1987; Hui *et al.* 1993) on that difficult background were included in our analysis. This left 27 planetaries in M101, 42 PN in M51, and 33 PN in M96 available for further analysis. Lists of all the planetaries found, their positions and magnitudes, and whether they are members of the statistical sample, are given in Tables 2, 3 and 4. Those PN that are part of the statistical samples are marked with an "S."

The PNLF distance to each galaxy and the formal uncertainty in each case were calculated by convolving the empirical function given in equation (1) with a photometric error vs. magnitude relation

derived from the output of DAOPHOT, and fitting the resultant curve to the complete sample of PN, via the method of maximum likelihood (Ciardullo *et al.* 1989a). In order to place our distances on the same system as previous PNLF distance determinations, we adopt $M^* = -4.48$, based on an M31 distance of 710 kpc (Welch *et al.* 1986), a foreground M31 reddening of $E(B-V) = 0.11$ (McClure & Racine 1969), and a Seaton (1979) reddening curve. With more recent values for M31's distance (770 kpc; Freedman & Madore 1990) and reddening ($E(B-V) = 0.08$; Burstein & Heiles 1984), the distances reported here would increase by $\sim 3\%$, or $+0.06$ mag in distance modulus. All our galaxy distances have assumed the foreground extinction values of Burstein & Heiles (1984).

The formal errors associated with our maximum-likelihood PNLF fits are $+0.04/-0.07$ mag for M101, $+0.06/-0.10$ mag for M51 and $+0.05/-0.07$ mag for M96. To compute the total error budget, these errors must be combined in quadrature with those associated with photometric zero point (0.02 mag), the filter response curve (0.04 mag), and the Galactic foreground extinction (0.05 mag; from Burstein & Heiles 1984). In addition, two systematic errors, which affect all PNLF measurements the same way, arise from the uncertain definition of the empirical PNLF (0.05 mag), and, of course, the distance to the calibration galaxy M31 (0.10 mag). The observed planetary nebula luminosity functions for the statistically complete samples of objects are displayed in Figure 1, along with the best fits for the empirical law. The luminosity functions are qualitatively similar to all the PNLF's seen in elliptical galaxies.

4. Results and Discussion

4.1. M101

The PNLF distance to M101 was reported in an earlier paper (Feldmeier, Ciardullo, & Jacoby 1996), so here we focus on additional results. The best-fitting distance for M101 (assuming no Galactic extinction; Burstein & Heiles 1984) is $(m-M)_0 = 29.36 \pm 0.15$, including all errors. With the newer M31 distance, this number increases to $(m-M)_0 = 29.42 \pm 0.15$. This distance assumes that the PNLF has not been affected by M101's internal extinction. If we adopt the mean measured extinction to Cepheids observed by the *Hubble Space Telescope* ($E(B-V) = 0.03$; Kelson *et al.*

1996), the distance modulus drops to within 1% of the *HST* Cepheid result ($(m-M)_0 = 29.34 \pm 0.16$). The issue of internal extinction is discussed in detail in §5.

Given M101's highly irregular background, it is extremely difficult to determine $\alpha_{2.5}$, the number of planetaries within 2.5 magnitudes of M^* normalized to the galaxy's bolometric luminosity. We can, however, estimate a lower limit to the number of planetaries expected within our detection threshold, and compare that to the number of PN actually found, assuming some value of $\alpha_{2.5}$. To do this, we first calculate the approximate B luminosity of M101, using the galaxy's total B magnitude of 8.31 (de Vaucouleurs *et al.* 1991; Buta *et al.* 1995), and our distance modulus of 29.42. If we assume the difference between M101's B and bolometric magnitudes is small, these numbers imply a total bolometric luminosity for the galaxy of $2 \times 10^{10} L_{\odot}$. If we then adopt a mean population age for the PN progenitors of 2×10^8 years, then the models of Renzini & Buzzoni (1986) imply a specific evolutionary flux of $\sim 1 \times 10^{-11}$ stars $\text{yr}^{-1} L_{\odot}^{-1}$. If it takes $\sim 25,000$ years for PN to fade 8 mag below M^* , equation (1) then implies that we should see ~ 125 PN in the brightest ~ 1 mag of the PNLF. We note that this estimate is extremely rough, as it depends on the uncertain bolometric luminosity of the galaxy, the assumption that all stars eventually become [O III] bright PN, and a young age for the PN progenitors. Nonetheless, our observations of 65 PN suggest that we are not sampling all the M101 PN brighter than our detection limit. This is to be expected, since the [O III] emission from H II regions interferes with finding planetaries in the spiral arms, and the high surface brightness prevents us from finding planetaries near the galaxy's nucleus. Moreover, it is possible that not all of M101's stars evolve through the [O III] bright PN phase. Ciardullo (1995) has found that the PN production rate in metal-rich, UV-bright elliptical galaxies can be a factor of ~ 4 less than predicted. Although no star-forming galaxy has ever been observed to be PN deficient, M101 is the first metal-rich spiral to be surveyed. Thus, although we are missing planetary nebulae, it is impossible to quantify exactly what our sampling rate is. However, these lack of detections should not affect the derived PNLF distance unless there are systematic differences between the detected and undetected PN.

4.1.1. Comparisons of M101 Distances

As there are so many distance estimates to this Sc galaxy, and given its well known importance for determining the Hubble constant, it is appropriate to compare our distance to M101 with distances derived from other techniques. We first compare our results to the Cepheid variables, which are thought to be the most reliable extragalactic distance indicator. From their inability to detect Cepheid variables photographically, Sandage & Tammann (1974a) first claimed an M101 distance modulus of $(m-M)_0 > 29.0$. Much later, Cook, Aaronson, & Illingworth (1986) used a CCD to detect 2 Cepheids in the R-band, and derived a preliminary distance modulus of ~ 29.2 . This was supplemented by observations of two additional Cepheids, and five Mira variable stars observed by Alves & Cook (1995), who found $(m-M)_0 = 29.08 \pm 0.13$, a value somewhat smaller than Cohen's (1993) Cepheid estimate of $(m-M)_0 = 29.4 \pm 0.15$. The most reliable Cepheid distance measurement, however, comes from Kelson *et al.* (1996) as part of the *Hubble Space Telescope* Distance Scale Key Project. Kelson *et al.* detected 29 Cepheids in the outer part of M101, and derived a distance modulus of $(m-M)_0 = 29.34 \pm 0.17$, with a mean Cepheid reddening of $E(B-V) = 0.03$. This distance measurement is in excellent agreement with our value.

We now briefly compare our PNLF distance to some other methods. Using the expanding photosphere method (EPM) on SN 1970G, Schmidt, Kirshner, & Eastman (1992) found a distance modulus to M101 of $(m-M)_0 = 29.34^{+0.28}_{-0.49}$. Though the errors are large, the agreement with both the PNLF method and the HST Cepheids is encouraging, and suggests that the EPM method is fundamentally sound. From a mean BRI Tully-Fisher relation, Pierce (1994) reported a rough distance modulus of $(m-M)_0 = 29.2 \pm 0.5$, also in good agreement with our result. Finally, M101 has been used as a testbed for using the brightest stars as distance indicators (Sandage 1983; Humphreys & Aaronson 1987). Though the errors in this method are thought to be large (Rozanski & Rowan-Robinson 1994), the assertion by Humphreys *et al.* (1986) that the distance modulus of M101 must be less than 28.4 because of the limits imposed by the intrinsic luminosities of M supergiants, seems to be incorrect. The distances to M101 given in the literature are listed in Table 5. For some comments on the earlier results, see de Vaucouleurs (1993).

The extremely good agreement between M101's *HST* Cepheid distance and our PNLF distance puts a strong limit on the systematic effect proposed by Bottinelli *et al.* (1991). Bottinelli *et al.* hypothesized that the true shape of the planetary nebula luminosity function has a power-law slope at the bright end, with no physical cutoff. Consequently, their model predicts that all PNLF distances have a systematic error, which is correlated with the absolute luminosity of the host galaxy. Bottinelli *et al.* parameterized this effect (their equation 3), as

$$\mu' = (0.4/\alpha')(M_g - M_g^0) + \mu_{true} \quad (3)$$

where M_g and M_g^0 are the absolute magnitudes of an unknown galaxy and of a galaxy where the value of M^* is known precisely, and $\alpha' = 1.6$. We can test this formula by calculating the predicted shift due to this supposed effect, and comparing it to our actual results. We follow the methodology of Bottinelli *et al.* (1991), and substitute M_B magnitudes for M_g and M_g^0 , even though this violates the equation above. The calibrator galaxy for the PNLF, the bulge of M31, has $B_T = 4.92$ (de Vaucouleurs 1958) with $A_B = 0.32$ (Burstein & Heiles 1984), and we assume a distance modulus to M31 of $(m-M)_0 = 24.42 \pm 0.12$ (Freedman & Madore 1990). If we adopt the Cepheid distance modulus to M101 of $(m-M)_0 = 29.34 \pm 0.16$ (Kelson *et al.* 1996), and use $B_T^0 = 8.31$ (de Vaucouleurs *et al.* 1991; Buta *et al.* 1995), then we find the expected error in our M101 distance is:

$$\mu' = -0.31 \pm 0.05 + \mu_{true} \quad (4)$$

Our derived distance of $(m-M)_0 = 29.42 \pm 0.15$, disagrees with this estimate by 0.39 ± 0.16 magnitudes. Even more significantly, if the M101 Cepheid distance is precisely correct, our PNLF distance is a slight overestimate. If the Bottinelli *et al.* hypothesis were true, we should underestimate the distance to M101 compared to the Cepheid distance. From the results above, the predicted shift of Bottinelli *et al.* is excluded with greater than 98% confidence. This, along with other studies in the Virgo and Fornax clusters, invalidates the Bottinelli *et al.* premise.

4.2. M51

The M51 system is a galaxy pair consisting of M51 (NGC 5194), an SBbc(s) II-III spiral, and NGC 5195, a satellite companion of type SB0 pec (Sandage & Tammann 1987). The main body of M51 has a higher surface brightness than M101 and a smaller inter-arm spacing, so planetary

detections in these areas are difficult. However, as Figure 2 shows, a substantial planetary nebula population exists in M51’s halo. Interestingly, the largest concentration of planetary nebulae is to the west of NGC 5195. Deep images of the M51 system show an increase in surface brightness in this region (for an example, see Burkhead 1978), but it is unknown whether the planetaries are related to NGC 5195, or are part of a halo population of M51. This pattern is most likely due to the tidal interaction of the two galaxies, but in theoretical studies (Toomre & Toomre 1972; Howard & Byrd 1990) this area has not been mentioned. Radial velocity measurements of these planetaries should provide an interesting dynamical constraint to the system.

The PNLF for this galaxy is plotted in Figure 1. The derived best-fitting distance to M51 (assuming no Galactic extinction; Burstein & Heiles 1984) is $(m-M)_0 = 29.56 \pm 0.15$, including all errors. With the improved M31 distance, our value increases to $(m-M)_0 = 29.62 \pm 0.15$. This result also assumes that internal extinction in the galaxy is insignificant. Since almost all of the PN are outside of the visible optical disk, this is likely to be a valid assumption (Giovanelli *et al.* 1994).

4.2.1. Comparisons of M51 Distances

Despite the well known nature of the M51 galaxy system and its importance, few distance determinations exist in the literature. In the past, most distances to this galaxy have been based on group membership, or an assumed value of the Hubble constant; these methods generally placed M51 near, or slightly more distant than M101 (Sandage & Tammann 1974a; Holmberg 1964). The only two direct measurements of M51’s distance prior to 1994 disagreed dramatically. The first, by Sandage & Tammann (1974b), placed M51 at $(m-M)_0 = 29.91$ based on the sizes of its H II regions; the second by Georgiev *et al.* (1990), put the galaxy at $(m-M)_0 = 29.2 \pm 0.20$ via the sizes of its young stellar associations. Fortunately, in the last year three new distance estimates have been made. Baron *et al.* (1996) used the spectral-fitting expanding atmosphere method (SEAM) on the type Ic SN 1994I, to derive a preliminary distance modulus of $(m-M)_0 = 28.9 + 5 \log(t_r/9 \text{ days}) \pm 0.5 \pm 0.7$, where t_r is the rise time of the bolometric light curve, the first set of uncertainties is due to the model, and the second set of uncertainties includes the effects of extinction. (They assume $E(B-V)_{SN} = 0.45$, and their best value for t_r is 9 days.) This distance is thought to be preliminary because of the sensitivity of the models to abundance stratification (Baron 1996). Similarly, Iwamoto *et al.* (1994)

derived a distance modulus to SN 1994I of $(m-M)_0 = 29.2 \pm 0.3$ from their theoretical calculations of exploding C + O stars. Unfortunately, both these distance determinations suffer from the fact that SN 1994I occurred in a dust lane close to the center of the galaxy, and thus the value of the extinction is highly uncertain (Richmond *et al.* 1996).

Perhaps the most reliable distance to M51 comes from surface brightness fluctuations found by Tonry (1996). The preliminary distance to NGC 5195 based on this method is $(m-M)_0 = 29.59 \pm 0.15$, in excellent agreement with our value. The distances to M51 are given in Table 6.

4.3. M96

M96 is an Sab(s)II galaxy in the Leo I group of galaxies. Leo I has been recognized as an important stepping stone to the Hubble constant as far back as Humason, Mayall, & Sandage (1956), and its brightest spiral, M96, has gained new attention due to the recent *Hubble Space Telescope* Cepheid measurements by Tanvir *et al.* (1995). In Figure 3, we plot the positions of M96's planetary nebulae candidates. Once again, the planetaries are detected at large galactocentric radii, far away from the high surface brightness regions of the galaxy. This is the most distant of the galaxies in this survey, and the data were taken under the poorest seeing conditions: only ~ 0.8 mag of the PNLF is sampled. Nevertheless, we derive a best-fitting distance to M96 (assuming a Galactic extinction of 0.015 mag; Burstein & Heiles 1984) of $(m-M)_0 = 29.85 \pm 0.15$, including all errors. With the improved distance to M31, this distance increases to $(m-M)_0 = 29.91 \pm 0.15$. As for M51, we make no correction for internal extinction as the amount of dust at large radii is likely to be small (Giovanelli *et al.* 1994).

4.3.1. Comparisons of M96 Distances

The Leo I group is a close-by, well-mixed galaxy group, containing two giant ellipticals (NGC 3377 and 3379), two SB0's (NGC 3384 and 3412), an Sab (NGC 3368), and an SBb (NGC 3351) galaxy. It is felt from many studies (Turner & Gott 1976; Huchra & Geller 1982; Geller & Huchra 1983; Vennik 1984; Tully 1988; Schneider 1989; Schneider *et al.* 1989) that these galaxies are at the same approximate distance. This allows us to compare our M96 distance to Leo I group distances found from other methods. Historically, these distances have ranged from as high as $(m-M)_0 = 31.18$

(Visvanathan 1979), to as low as $(m-M)_0 = 29.84$ (Tonry 1991). We now focus on several selected distance indicators to the group.

The Tully-Fisher relation has been partially calibrated on galaxies near the Leo I group. Specifically, the nearby Leo triplet, which consists of NGC 3623, 3627, and 3628, has been used by Aaronson & Mould (1983) as an infrared Tully-Fisher calibrator. Their group distance modulus of $(m-M)_0 = 29.84 \pm 0.25$, with an additional ~ 0.2 mag systematic uncertainty, is in good agreement with our value, though it is problematic whether this triplet is at the same distance as the Leo I group.

The globular cluster luminosity function (GCLF) distance indicator has also been used on galaxies in the Leo I group. By summing the globular clusters found in NGC 3377 and NGC 3379, and assuming a Milky Way GCLF peak at $M_B^0 = -6.84 \pm 0.17$, Harris (1990) estimated the group's distance to be $(m-M)_0 = 30.19 \pm 0.43$. This result is also in approximate agreement with our M96 result, especially considering the method's large error bars.

Another standard candle that has recently been used in the Leo I Group is the tip of the red giant branch. By identifying the abrupt discontinuity in the luminosity function of resolved stars in NGC 3379, Sakai *et al.* (1996) have estimated a distance to the group of $(m-M)_0 = 30.20 \pm 0.14$. Again, this is consistent with the results from planetary nebulae.

A technique that has been compared frequently to the PNLF is the surface brightness fluctuations (SBF) method. This method, pioneered by Tonry & Schneider (1988), has been used on a large number of early-type galaxies, including NGC 3377, 3379, and 3384 (Tonry *et al.* 1990; Tonry 1991; Ciardullo, Jacoby, & Tonry 1993). The best-fitting SBF distance moduli for these galaxies are $(m-M)_0 = 29.94 \pm 0.08$, $(m-M)_0 = 29.87 \pm 0.07$, and $(m-M)_0 = 29.88 \pm 0.12$ respectively, in excellent agreement with our distance to M96. A discussion of PNLF versus SBF distances is given in Ciardullo, Jacoby, & Tonry (1993).

A critical test for the PNLF method is the comparison of our M96 distance with the PNLF measurements to the other galaxies of the group. Our M96 distance modulus of $(m-M)_0 = 29.91 \pm 0.15$ is, within the errors, identical to that previously measured to the three early-type galaxies NGC 3377, 3379, and 3384 (distance moduli of 30.13 ± 0.17 , 30.02 ± 0.16 , and 30.09 ± 0.15 , respectively). This agreement further reinforces the conclusion that PNLF distances have little or no

dependence on galaxy Hubble type (cf. Ciardullo, Jacoby, & Harris 1991; Jacoby, Ciardullo, & Harris 1996).

Finally, we look at the *Hubble Space Telescope* Cepheid distances to the group. There are two Leo I galaxies with *HST* Cepheid measurements: M96 and M95 (NGC 3351). Unfortunately, these two measurements yield conflicting results. From the light curves of 45 Cepheids found in M95, Graham *et al.* (1996) estimate a group distance modulus of $(m-M)_0 = 30.01 \pm 0.19$, in good agreement to our value. However, the initial results derived from the analysis of seven Cepheids in M96 (Tanvir *et al.* 1995) imply a distance modulus of $(m-M)_0 = 30.32 \pm 0.16$, 1.9σ larger than the PNLF distance. This PNLF/Cepheid distance discrepancy is the largest to date, and it occurs in the most distant galaxy with both a PNLF and Cepheid distance determination. If the M96 Cepheid distance is correct, it may be the first evidence for a change of M^* with stellar population. However, it is difficult to understand why such an effect is not seen in M101 or M51.

Alternatively, Graham *et al.* claim that the *V*-band Cepheid period-luminosity relations found for M95 and M96 are consistent, and that only the *I*-band relations are different. Thus, the only difference between the two numbers is the derived values of the absorption corrections. Madore & Freedman (1991) state that in order to obtain both an accurate distance and reddening estimate to a galaxy, two or three dozen Cepheids are needed. Since only seven Cepheids are used to estimate the Cepheid distance to M96, (and only 3 *I*-band measurements were obtained), it is possible that the Cepheid distance to this galaxy has been overestimated. In Table 7, we list the distances to Leo I group galaxies given in the literature.

5. The Effect of Dust

In all the above distance determinations, we ignored the presence of dust within the target galaxy. Several lines of reasoning suggest this is reasonable. First, our method for identifying a statistically complete sample of planetary nebulae selects against objects superposed near regions of strong extinction. By excluding objects that have highly variable backgrounds, we select against planetary nebulae that are close to patches of dust.

Second, there is evidence from other studies that the disks of spiral galaxies are not opaque, though there is considerable debate on this point (for opposing views, see Valentijn 1990 and Disney,

Davies, & Phillips 1989). Giovanelli *et al.* (1994), through a careful study of dust in a well-defined sample of Sc galaxies, has found that extinction is almost non-existent two or three scale lengths away from the center. In M96, all but 14 of the planetaries have projected galactocentric distances greater than three scale lengths (Kent 1985); in M51, virtually all of the identified PN are well outside the main body of the galaxy. Additionally, Rowan-Robinson (1992) has fit dust models to IRAS data in many disk galaxies, and has found that the amount of extinction averaged over the entire disk is small, with $A_V < 0.1$ mag except near the galactic centers. His dust models of M101 and M51 imply mean differential extinctions of $E(B-V) = 0.0056$ and 0.013 , respectively. Thus, again, the extinction applicable to our PN population appears to be small.

A third justification for neglecting the effects of internal extinction comes from considering the positions of planetary nebulae within our own Galaxy and other spiral galaxies. In the Milky Way, planetary nebulae have a higher vertical scale height than the dust (Allen 1973). Planetary nebulae are also seen at high z distances in the edge-on Sb spirals NGC 891 and NGC 4565 (Ciardullo, Jacoby, & Harris 1991; Jacoby, Ciardullo, & Harris 1996). Therefore, it is likely that a substantial fraction of our PN candidates lie above and below the dust layers of the target galaxies. Since only those planetaries below the dust will be extinguished, a thin layer of extinction should only distort the faint end of the PNLF by dimming objects on the far side of the galaxy; the computed distance, which comes from the brightest objects in front of the dust, should remain unaffected. This hypothesis can be tested quantitatively by first assuming that the dust and planetaries in M101 have the same vertical scale heights as in our Milky Way galaxy, and then modeling the PNLF expected from such a distribution. By varying the total amount of extinction at $\lambda 5007$ perpendicular to the disk, we can compute a dust-altered PNLF and fit this function to our M101 data. The results are plotted in Figure 4. As expected, dust has little effect on our PNLF distances: the derived distance modulus is always within 0.1 mag of the result obtained by assuming no internal extinction. This offset is comparable to our internal error bars.

Finally, we can ask what the worst case scenario for dust should be. If all of our planetaries are Pop I disk objects, they should suffer a comparable amount of extinction to that of Cepheid variables. In the *Hubble Space Telescope* Cepheid observations of M101, Kelson *et al.* (1996) derived a mean

$E(B-V)$ from their observations of 0.03 mag. Using a Seaton (1979) reddening curve, the extinction in [O III] would then be $A_{5007} = 0.11$ mag, similar to that estimated above.

In conclusion, it is likely that the effect of dust on the PNLF in face-on spirals is minimal, and certainly no more than ~ 0.1 mag. Hence we make no correction for internal extinction at this time. In the future, this assumption can be put to a direct observational test by observing the Balmer lines in our large sample of planetaries.

6. Detection of Supernovae

In previous PNLF studies of elliptical galaxies, searches have been made for the remnants of historical supernovae, since these objects may contribute to the population of overluminous [O III] $\lambda 5007$ sources (Jacoby, Ciardullo, & Harris 1996). Interestingly, none of these remnants have been detected, either because the remnants are still too dense to emit at $\lambda 5007$, or because the local interstellar medium is so sparse that the shells have already expanded to an undetectable low density (Jacoby, Ciardullo, & Ford 1990a). In our sample of spiral galaxies, there have been five historical supernovae: three in M101 (SN 1909A, 1951H, and 1970G) and two in the M51 system (SN 1945A and 1994I). To assess the effect of recent supernovae on the bright end of the PNLF, we searched our data for the remnants of these explosions. SN 1909A was too far west of M101's nucleus to be included on our images, but the other four supernovae are contained within our survey fields. We discuss each supernova below.

6.1. SN 1970G

SN 1970G, a type II-L supernova, has been detected in the radio (Gottesmann *et al.* 1972), and recently has been recovered in the optical by Fesen (1993). Fesen's spectra show little or no [O III] emission related to the supernova. The images of the on-band and off-band frames are displayed in Figure 5, and should be compared with the R -band image given in Fesen's paper. As can be seen in the figure, the supernova is detectable on the off-band image, but there is no corresponding emission at $\lambda 5007$. We did not recover the supernova in our R -band exposure, but since the seeing on the frame was poor and our exposure time was much shorter than that of Fesen, the two results are still consistent. The SN appears to be a continuum source, but not a source of [O III] $\lambda 5007$ emission.

6.2. SN 1951H

The type II supernova, SN 1951H was originally discovered by Humason and announced as a supernova by Bowen (1951). The supernova lies just to the east of NGC 5462, a giant H II region in one of the spiral arms of M101. In Figure 6, we display the region surrounding NGC 5462. From a visual inspection of a supernova image (Abell 1975), it appears that SN 1951H's reported nuclear offset of $350''$ north and $45''$ east (Barbon, Cappellaro, & Turatto 1989) is incorrect; the object appears to be located approximately $8''$ east, and $3''$ north of the reported position. No [O III] emission is seen at this location, though there does appear to be at least two continuum sources in the area. Further study is not possible at this time, due to the positional uncertainty: there are no recent optical measurements, and the object has not been recovered in the radio (Allen, Goss, & van Woerden 1973). This problem can, however, be resolved in the future via astrometric measurements of the original photographic plates.

6.3. SN 1994I

SN 1994I, a type Ic supernova near M51's nucleus, was discovered on 1994 April 2, by several sets of observers. This object has been extremely well studied in the optical (for a summary, see Richmond *et al.* 1996), and also has a radio detection (Rupen *et al.* 1994). Using images kindly provided to us by Michael Richmond and Schuyler Van Dyk, we searched for evidence of the supernova in our images. The supernova was detected on all our frames, which suggests the object is still in decline from the initial explosion. At the time of our survey (~ 1 yr after maximum), there was no evidence for nebular activity.

6.4. SN 1945A

SN 1945A, a type I supernova, exploded in the satellite galaxy of M51, NGC 5195. The recorded position of the event was $6''$ west and $4''$ south of the galaxy nucleus. No point source appears at these coordinates, either in the continuum, or in [O III]. Due to the lack of accurate astrometric coordinates for this object, we cannot draw any further conclusions.

6.5. Discussion

In our sample of four historical supernovae, we detected only one in our [O III] $\lambda 5007$ filter, SN 1994I, but this object is clearly a continuum source still in decline from the initial explosion. How does this agree with previous results? Currently, there are at least ten historical extragalactic supernovae that have been optically recovered 3 years or more after the initial explosion (for a review, see Leibundgut 1994). Most of these objects do have strong [O III] emission, with SN 1970G being the exception. So far, the optical emission from historical supernovae has always been accompanied by corresponding radio emission; this is thought to be due to the interaction of the supernova shock wave with circumstellar matter released previously in the star's lifetime (Chevalier 1982, 1984). This naturally explains why only historical supernovae of type II and type I b/c have been recovered in the optical and radio. Looking at our particular cases, we see that SN 1945A was a type I, and thus should not be emitting in [O III] $\lambda 5007$. Similarly, SN 1951H has not been detected in the radio, and so it, too, may not be undergoing an interaction with a circumstellar medium. Finally, although SN 1970G does have a radio detection, the object has never been seen to have [O III] lines, so it should also be undetectable in our survey.

From other studies, the rate of recovery of historical supernovae is low. Out of the six supernovae which have occurred in NGC 6946 in the past 75 years, only one remnant has been detected (Fesen & Becker 1990). Similarly, only one of the 6 historical supernovae of M83 has been recovered (Long, Blair, & Krzeminski 1989). Thus, our non-detection of supernovae is consistent with other searches.

How does the presence of supernova remnants affect the PNLF as a distance indicator? With the exception of SN 1957D (Long, Blair, & Krzeminski 1989), [O III] $\lambda 5007$ emission is always accompanied by strong $H\alpha$ emission. Thus our $H\alpha$ frames should allow us to remove supernova remnants in the same way as H II regions. Other ways of discriminating luminous PN from supernova remnants include looking for radio emission or the presence of shock diagnostic emission lines, such as [S II] $\lambda\lambda 6716, 6731$. Finally, we note that [O III] $\lambda 5007$ has not been detected in any historical type Ia SN event (Leibundgut 1994). Thus, the PNLF in normal elliptical galaxies should have no contamination from supernova remnants.

7. The Cepheid - PNLF Comparison

With the addition of M101 and M96, there are now seven galaxies with both a PNLF and Cepheid distance determination. In addition, there are three galaxy groups where an indirect comparison can be made: the NGC 1023 Group (Silbermann *et al.* 1996; Ciardullo, Jacoby, & Harris 1991), the Virgo Cluster (Ferrarese *et al.* 1996; Saha *et al.* 1996; Jacoby, Ciardullo, & Ford 1990a), and the Fornax Cluster (Freedman 1996; McMillan, Ciardullo, & Jacoby 1993). In Figure 7 and Table 8, we compare the PNLF and Cepheid distances to these objects. The error bars given in the table are those quoted by the authors, with the systematic uncertainties common to both methods removed. For the PNLF technique, these systematic uncertainties include the 0.1 mag error associated with the distance to M31, and the 0.05 mag uncertainty in the definition of the PNLF; for the Cepheid measurements, the ~ 0.1 mag uncertainty associated with the distance and reddening to the Magellanic Clouds has been excluded. To place the PNLF on the same scale as the Cepheids, we have adopted an M31 distance of 770 kpc (Freedman & Madore 1990), and a foreground reddening of $E(B-V) = 0.08$ (Burstein & Heiles 1984). In the case of NGC 5253 only, a correction to its distance might be needed, if the galaxy is extremely metal poor (Ciardullo & Jacoby 1992). There is evidence that the metallicity of NGC 5253 (Melnick *et al.* 1992; Pagel *et al.* 1992; Walsh & Roy 1989) warrants a correction as large as -0.28 mag, but since others (e.g., Campbell 1992; Storch-Bergmann *et al.* 1994) report near-LMC metallicities, it is unclear whether this correction should be used. We have chosen not to apply a distance correction to NGC 5253; were we to do so, the discrepancy between the PNLF and Cepheid distances to the galaxy would change from $+0.4\sigma$ to -0.5σ .

As can be seen in the figure, there is extremely good agreement over two orders of magnitude in the derived distances: the only galaxy whose Cepheid distance varies by more than 1σ from the PNLF distance is M96. In the bottom of Figure 7, we plot the fractional residuals between the Cepheid and PNLF distances. Note that, with the exception of M96, the scatter about the zero line is completely consistent with the error bars. Moreover, if we were to adopt the Leo I Group distance of Graham *et al.* (1996), rather than that of Tanvir *et al.* (1995), M96, too, would agree within the errors.

The data presented in Table 8 affords us an opportunity to check the zero point calibration of the PNLF by computing the mean value of $\Delta = (m - M)_{\text{PNLF}} - (m - M)_{\text{Cepheid}}$ for our

sample of galaxies. From the six galaxies (other than M31) with both Cepheid and PNLF distance measurements, we find $\langle \Delta \rangle$ of -0.01 (weighted) and $\langle \Delta \rangle = +0.01$ (unweighted). If the Graham *et al.* Cepheid distance to M95 is substituted for the Tanvir *et al.* M96 distance, this offset changes to $\langle \Delta \rangle = +0.03$ (weighted) and $\langle \Delta \rangle = +0.06$ (unweighted). Finally, if the results from the NGC 1023 Group, the Fornax Cluster, and the Virgo Cluster are folded in, with an assumed intracluster scatter of ± 1 Mpc, then $\langle \Delta \rangle = +0.02$ (weighted) and $\langle \Delta \rangle = +0.03$ (unweighted). This excellent agreement is yet another confirmation of the robustness of the PNLF method, and demonstrates that our calibration of M^* in M31 is certainly within the quoted errors.

The agreement between the PNLF and Cepheid distances also places a possible constraint on theories for the dependence of the planetary nebula luminosity function with population age. Models by Jacoby (1989), Méndez *et al.* (1993), and Han, Podsiadlowski, & Eggleton (1994) all suggest that a population of PN derived from young, massive stars, should have a value of M^* brighter than that seen in an old stellar population. Specifically, Méndez *et al.* (1993) predict a difference of ~ 0.6 mag between the PNLF cutoff in a population with a constant star formation rate, and that in an old elliptical galaxy.

This effect is not seen in our data, except possibly in M96. Indeed, in the case of M101, if there is any effect at all, it goes in the wrong direction: our distance to M101 is slightly larger than that derived from the Cepheids, and this implies a slightly fainter value for M^* . A possible explanation for the apparent lack of an age dependence may lie in our selection criteria for planetary nebulae. In order to avoid contamination by H II regions, our PN survey preferentially identified objects away from star forming regions. Consequently, we may be discriminating against the highest mass PN. In addition, the (small) effects of internal extinction within the surveyed spirals may also work to mask a population effect. Nevertheless, the results are consistent with the PNLF analysis of Jacoby, Walker, & Ciardullo (1990b) for the Large Magellanic Cloud. No age effect was seen in that galaxy, either. If this lack of an age effect is real, and not due to a selection effect, it implies either that a) the PN progenitors in late-type spirals have similar ages to those in ellipticals and spiral bulges, b) the initial-to-final mass relationship for post-asymptotic branch stars is nearly independent of progenitor mass, or c) high mass progenitors conspire to be relatively faint in [O III] $\lambda 5007$, perhaps due to their short evolutionary time scales (*e.g.*, Schönberner 1981; 1983), high nitrogen-to-oxygen abundance

ratio (Kaler & Jacoby 1991), or differences in geometry (Méndez 1996). However, more tests with spiral galaxies will be needed to test this hypothesis.

8. Conclusion

We have searched for planetary nebulae in the spiral galaxies M101, M51 and M96, and obtained distance moduli of $(m-M)_0 = 29.42 \pm 0.15$, $(m-M)_0 = 29.62 \pm 0.15$, and $(m-M)_0 = 29.91 \pm 0.15$ respectively, using the planetary nebula luminosity function. The M101 distance agrees extremely well with the *HST* Distance Scale Key Project Cepheid measurement, and the M51 distance is in excellent agreement with the distance determined by surface brightness fluctuations. The M96 distance is consistent with other PNLF measurements in the Leo I group, and the Leo I distance found by the *HST* Distance Scale Key Project, but disagrees with the Cepheid distance found by Tanvir *et al.* The success of our observations implies that PNLF measurements are an effective ground-based alternative to *Hubble Space Telescope* measurements of Cepheid light curves.

We thank M. Bershady and R. Wade for comments on an earlier version of this paper, and E. Baron for comments on the SEAM distance to M51. We especially thank M. Richmond and S. van Dyk for the use of their SN 1994I images in our supernova search. We also thank the referee, L. Stanghellini, for several suggestions that improved this paper. This work was supported in part by NASA grant NAGW-3159.

TABLE 1

Record of Observations

Object Name	Date	Filter	Exposure (sec)	Number of Exposures
M 101	1995 April 5	5027/30	3600	2
M 101	1995 April 5	5312/267	540	2
M 101	1995 April 5	6586/72	900	1
M 96	1995 April 6	5027/30	3600	3
M 96	1995 April 6	5312/267	540	3
M 96	1995 April 7	6586/72	900	3
M 96	1995 April 7	5312/267	540	2
M 51	1995 April 7	5027/30	3600	2
M 51	1995 April 7	5312/267	540	2
M 101	1995 April 8	6563/75	900	4
M 101	1995 April 8	<i>R</i> band	60	4
M 101	1995 April 11	6563/75	900	2
M 101	1995 April 11	<i>R</i> band	60	2
M 51	1995 April 11	6563/75	900	6
M 51	1995 April 11	R band	60	6

TABLE 2
M101 PLANETARY NEBULAE

ID	$\alpha(2000)$	$\delta(2000)$	$R_{iso}(')$	m_{5007}	Notes	ID	$\alpha(2000)$	$\delta(2000)$	$R_{iso}(')$	m_{5007}	Notes
1	14 02 40.45	54 13 55.4	8.4	24.97	S	34	14 03 03.52	54 21 48.1	1.6	25.72	
2	14 02 48.53	54 16 19.0	5.8	24.99	S	35	14 02 38.80	54 27 21.1	8.1	25.73	S
3	14 03 09.80	54 21 05.5	0.4	25.02		36	14 02 38.30	54 20 20.6	5.0	25.74	S
4	14 02 54.19	54 25 08.4	5.0	25.17	S	37	14 03 20.39	54 20 06.5	1.4	25.77	
5	14 02 39.78	54 16 13.7	6.7	25.19	S	38	14 02 47.56	54 27 52.1	7.8	25.82	S
6	14 02 54.30	54 25 28.5	5.3	25.21	S	39	14 03 24.24	54 28 00.8	7.3	25.83	S
7	14 03 21.89	54 25 47.8	5.1	25.25		40	14 02 19.82	54 24 40.9	8.5	25.83	S
8	14 02 58.71	54 16 37.5	4.7	25.25		41	14 03 00.58	54 22 37.2	2.4	25.85	
9	14 03 12.33	54 28 16.5	7.3	25.33	S	42	14 03 02.68	54 25 57.4	5.2	25.87	S
10	14 03 14.16	54 20 35.2	0.4	25.34		43	14 02 26.16	54 18 42.0	7.1	25.88	
11	14 03 04.25	54 14 44.3	6.3	25.35	S	44	14 03 10.12	54 27 39.7	6.8	25.88	S
12	14 02 21.48	54 21 07.9	7.4	25.38	S	45	14 03 46.40	54 25 21.6	6.7	25.88	S
13	14 03 16.53	54 19 26.8	1.6	25.41		46	14 03 36.67	54 19 34.0	3.8	25.89	S
14	14 03 28.55	54 23 02.1	3.2	25.44		47	14 02 56.64	54 24 45.7	4.5	25.90	
15	14 03 04.55	54 19 56.6	1.5	25.44		48	14 03 18.02	54 19 33.8	1.6	25.92	
16	14 03 20.60	54 24 28.0	3.7	25.45		49	14 02 41.66	54 25 07.5	6.1	25.93	
17	14 02 40.26	54 24 11.4	5.7	25.46	S	50	14 02 36.10	54 14 09.2	8.6	25.94	
18	14 03 23.78	54 16 52.2	4.4	25.46		51	14 03 37.21	54 23 47.3	4.6	25.96	
19	14 02 22.58	54 24 22.0	8.0	25.47	S	52	14 03 22.49	54 16 03.0	5.1	25.96	
20	14 03 12.05	54 21 10.6	0.3	25.54		53	14 02 32.32	54 19 31.0	6.0	25.97	
21	14 03 10.40	54 20 18.2	0.7	25.55		54	14 03 30.52	54 26 04.9	5.8	25.98	
22	14 02 36.34	54 25 16.9	6.8	25.55	S	55	14 03 43.34	54 17 19.8	5.8	26.01	
23	14 03 23.66	54 21 21.3	1.7	25.58		56	14 03 52.50	54 27 41.2	8.9	26.06	
24	14 03 00.48	54 16 50.3	4.4	25.59		57	14 03 23.44	54 13 46.4	7.3	26.12	
25	14 03 17.12	54 14 59.4	6.0	25.59	S	58	14 02 30.58	54 18 24.4	6.6	26.13	
26	14 02 34.23	54 24 37.4	6.7	25.60	S	59	14 03 42.64	54 25 41.7	6.5	26.14	
27	14 03 34.63	54 25 03.7	5.3	25.61	S	60	14 02 44.60	54 21 08.0	4.1	26.17	
28	14 02 21.59	54 21 09.0	7.4	25.65	S	61	14 02 41.77	54 21 44.9	4.5	26.18	
29	14 03 08.12	54 25 25.1	4.5	25.66	S	62	14 03 22.39	54 20 05.3	1.7	26.35	
30	14 02 53.50	54 13 24.9	8.0	25.67	S	63	14 03 22.32	54 22 24.8	2.1	26.37	
31	14 03 19.21	54 19 50.8	1.5	25.68		64	14 02 39.89	54 22 58.3	5.2	26.39	
32	14 03 34.07	54 24 41.1	4.9	25.71	S	65	14 03 05.84	54 25 36.7	4.8	26.43	
33	14 03 07.28	54 19 02.8	2.0	25.71							

TABLE 3
M51 PLANETARY NEBULAE

ID	$\alpha(2000)$	$\delta(2000)$	$R_{iso}(')$	m_{5007}	Notes	ID	$\alpha(2000)$	$\delta(2000)$	$R_{iso}(')$	m_{5007}	Notes
1	13 29 50.53	47 06 26.7	5.3	25.15	S	33	13 30 01.04	47 04 48.4	7.1	25.83	S
2	13 30 03.48	47 17 58.6	6.5	25.34	S	34	13 29 54.83	47 18 30.7	6.8	25.85	S
3	13 30 16.64	47 14 02.0	4.7	25.35	S	35	13 30 07.70	47 16 22.7	5.3	25.86	
4	13 29 38.17	47 17 38.9	6.4	25.36	S	36	13 29 43.74	47 16 13.6	4.8	25.88	S
5	13 29 22.94	47 17 25.8	7.6	25.38	S	37	13 29 30.58	47 14 36.0	4.7	25.90	S
6	13 29 44.74	47 09 14.7	2.8	25.38		38	13 29 51.00	47 16 06.5	4.4	25.93	
7	13 29 29.07	47 15 10.8	5.3	25.39	S	39	13 29 45.54	47 17 29.8	5.9	25.97	
8	13 29 48.62	47 16 38.1	5.0	25.42	S	40	13 29 17.08	47 15 21.3	7.0	25.98	S
9	13 30 14.69	47 14 43.9	4.8	25.44	S	41	13 30 05.13	47 17 37.4	6.3	26.00	S
10	13 29 48.65	47 17 22.3	5.7	25.48	S	42	13 29 48.23	47 17 19.2	5.7	26.00	
11	13 29 57.05	47 17 30.8	5.9	25.51		43	13 30 12.48	47 14 08.2	4.2	26.00	S
12	13 29 38.90	47 08 04.1	4.3	25.52		44	13 29 46.41	47 06 54.3	4.9	26.02	S
13	13 29 36.95	47 17 26.4	6.3	25.54	S	45	13 29 43.63	47 15 48.5	4.4	26.03	
14	13 29 28.71	47 17 20.1	6.9	25.55	S	46	13 30 08.04	47 16 19.9	5.3	26.03	
15	13 29 35.56	47 16 42.3	5.8	25.55	S	47	13 29 50.34	47 05 37.9	6.1	26.08	S
16	13 29 36.56	47 07 06.3	5.3	25.62	S	48	13 29 23.90	47 15 02.3	5.9	26.08	S
17	13 29 47.78	47 15 57.6	4.3	25.62	S	49	13 29 53.10	47 05 43.7	6.0	26.09	S
18	13 29 48.96	47 17 24.1	5.7	25.62	S	50	13 29 44.50	47 16 04.5	4.6	26.15	S
19	13 30 00.33	47 17 09.4	5.6	25.63		51	13 29 51.03	47 18 34.9	6.9	26.16	S
20	13 29 50.08	47 17 12.6	5.5	25.65	S	52	13 29 15.94	47 13 00.0	6.3	26.17	S
21	13 29 36.80	47 08 33.7	4.1	25.66		53	13 29 50.83	47 17 20.5	5.7	26.17	S
22	13 29 34.15	47 17 39.7	6.7	25.66	S	54	13 29 55.09	47 18 59.8	7.3	26.21	
23	13 29 46.30	47 17 10.9	5.6	25.68		55	13 29 54.44	47 16 20.6	4.7	26.24	
24	13 29 45.75	47 15 30.9	4.0	25.68	S	56	13 29 23.19	47 17 14.3	7.4	26.25	S
25	13 29 30.91	47 15 47.2	5.5	25.68	S	57	13 30 08.06	47 17 55.0	6.8	26.28	S
26	13 29 29.74	47 16 31.6	6.2	25.68	S	58	13 29 43.96	47 05 51.2	6.0	26.29	S
27	13 30 05.59	47 07 18.7	4.9	25.69	S	59	13 29 46.87	47 05 35.6	6.2	26.35	
28	13 29 42.29	47 18 19.4	6.8	25.70	S	60	13 29 45.34	47 06 33.4	5.3	26.37	
29	13 29 39.92	47 15 12.5	4.1	25.70	S	61	13 30 33.80	47 13 32.6	7.2	26.39	
30	13 29 40.82	47 09 04.8	3.3	25.74		62	13 30 10.86	47 17 12.1	6.3	26.44	
31	13 29 59.71	47 16 59.2	5.4	25.77		63	13 29 25.64	47 17 11.9	7.1	26.47	
32	13 29 42.33	47 18 53.1	7.4	25.81	S	64	13 30 19.83	47 13 09.0	4.8	26.94	

TABLE 4
M96 PLANETARY NEBULAE

ID	$\alpha(2000)$	$\delta(2000)$	$R_{iso}(')$	m_{5007}	Notes	ID	$\alpha(2000)$	$\delta(2000)$	$R_{iso}(')$	m_{5007}	Notes
1	10 47 01.80	11 51 24.1	4.5	25.50	S	38	10 46 40.84	11 48 38.8	1.3	26.12	
2	10 46 47.77	11 50 53.5	1.8	25.52	S	39	10 46 44.91	11 45 01.4	4.2	26.14	S
3	10 46 47.96	11 46 48.2	2.4	25.53	S	40	10 46 36.46	11 47 22.4	2.9	26.15	S
4	10 46 48.94	11 47 53.2	1.5	25.53		41	10 46 54.64	11 48 54.3	2.2	26.16	
5	10 46 44.55	11 44 12.0	5.0	25.57	S	42	10 46 54.30	11 46 49.6	3.1	26.18	S
6	10 46 45.10	11 48 03.5	1.1	25.59		43	10 46 22.61	11 45 40.9	6.7	26.19	S
7	10 46 40.77	11 48 49.4	1.3	25.62		44	10 46 51.18	11 52 48.9	3.9	26.19	S
8	10 46 41.16	11 48 24.6	1.4	25.64		45	10 47 11.39	11 49 12.3	6.3	26.20	S
9	10 46 36.29	11 47 26.2	2.9	25.65	S	46	10 46 34.15	11 45 54.5	4.3	26.22	
10	10 46 40.71	11 45 19.0	4.1	25.70	S	47	10 46 36.64	11 52 39.0	4.1	26.27	
11	10 46 44.61	11 44 27.1	4.7	25.73	S	48	10 46 41.01	11 46 00.3	3.4	26.28	
12	10 46 48.56	11 49 23.5	0.7	25.73		49	10 46 51.48	11 51 46.2	2.9	26.28	
13	10 46 45.29	11 52 38.0	3.5	25.74	S	50	10 46 48.94	11 44 57.1	4.3	26.28	
14	10 46 47.58	11 50 44.6	1.6	25.75		51	10 46 47.19	11 47 24.0	1.8	26.28	
15	10 46 42.65	11 52 29.0	3.4	25.75	S	52	10 46 44.24	11 54 22.6	5.2	26.30	
16	10 46 42.71	11 53 17.0	4.2	25.77	S	53	10 46 38.13	11 54 55.8	6.1	26.31	
17	10 46 54.82	11 47 36.2	2.7	25.82	S	54	10 46 44.89	11 50 42.4	1.5	26.31	
18	10 46 52.49	11 47 37.7	2.2	25.83		55	10 46 45.29	11 53 59.8	4.8	26.34	
19	10 46 26.40	11 48 22.2	4.8	25.90	S	56	10 46 55.17	11 46 46.6	3.3	26.35	
20	10 46 39.98	11 47 32.9	2.2	25.91	S	57	10 46 43.75	11 52 43.6	3.6	26.38	
21	10 46 52.14	11 48 57.8	1.6	25.94	S	58	10 46 56.46	11 47 57.4	2.9	26.39	
22	10 46 55.33	11 44 58.3	4.8	25.95	S	59	10 46 43.63	11 51 05.9	2.0	26.41	
23	10 46 46.19	11 52 51.1	3.7	25.96	S	60	10 46 47.46	11 51 26.6	2.3	26.41	
24	10 46 55.66	11 47 19.9	3.0	25.96	S	61	10 46 46.21	11 47 20.9	1.8	26.44	
25	10 46 42.74	11 50 43.5	1.7	25.96		62	10 46 43.17	11 45 19.6	3.9	26.48	
26	10 46 51.88	11 47 47.0	2.0	25.97		63	10 46 43.91	11 54 03.2	4.9	26.48	
27	10 46 37.98	11 47 08.6	2.8	26.00	S	64	10 46 50.19	11 47 07.8	2.3	26.48	
28	10 47 00.30	11 46 08.8	4.7	26.01	S	65	10 46 59.52	11 49 09.1	3.3	26.55	
29	10 46 53.69	11 46 33.8	3.2	26.02	S	66	10 46 50.44	11 44 46.2	4.6	26.56	
30	10 47 04.80	11 52 39.0	5.8	26.03	S	67	10 46 43.13	11 55 39.4	6.5	26.59	
31	10 46 44.78	11 47 09.4	2.0	26.04	S	68	10 46 50.08	11 47 21.5	2.1	26.60	
32	10 46 46.21	11 44 39.5	4.5	26.07	S	69	10 46 35.74	11 48 53.3	2.5	26.62	
33	10 46 47.85	11 45 47.4	3.4	26.07	S	70	10 46 50.70	11 47 55.8	1.7	26.66	
34	10 46 42.95	11 51 04.5	2.0	26.08		71	10 46 58.43	11 47 59.1	3.3	26.70	
35	10 46 44.70	11 46 40.0	2.5	26.09	S	72	10 46 47.58	11 45 08.0	4.1	26.73	
36	10 46 51.86	11 46 21.3	3.2	26.10	S	73	10 47 02.24	11 55 38.1	7.6	26.91	
37	10 46 42.36	11 45 26.6	3.8	26.10	S	74	10 46 43.34	11 55 52.9	6.7	27.03	

TABLE 5

Distances to M101				
Year	Author	Method and Data	$(m-M)_0$	σ
1974a	Sandage & Tammann	Multiple Methods	29.3	0.3
1975	de Vaucouleurs	Group Membership	28.71	
1976	Sandage & Tammann	Multiple Methods	29.08	0.3
1976	Jaakkola & Le Denmat	Revision of S&T (1974b, 1976)	28.56	
1976	Bottinelli & Gouguenheim	Revision of S&T (1974b, 1976)	28.75	
1977	Melnick	Velocity Dispersion in H II Regions	28.7	0.6
1978	de Vaucouleurs	Group Membership	28.5	0.3
1979a	de Vaucouleurs	Revision of Melnick (1977)	28.08	0.4
1979b	de Vaucouleurs	Luminosity index	27.57	0.3
1979b	de Vaucouleurs	Type II SNe	27.60	
1980	Wray & de Vaucouleurs	Brightest Superassociation	27.76	0.6
1980	Capaccioli & Fasano	Revision of S&T (1974b, 1976)	28.8	0.3
1982	Lawrie & Kwitter	Largest H II ring	28.18	0.28
1983	Sandage	Brightest blue irreg. variables	29.2	
1983	Sandage	Brightest red supergiants	29.2	
1983	Humphreys & Strom	Brightest M Supergiants	28.6	0.3
1984	Bottinelli <i>et al.</i>	B-band T-F relation	28.7	
1985	Bottinelli <i>et al.</i>	B-band T-F relation	28.4	
1986	Humphreys <i>et al.</i>	Brightest M Supergiants	28.4	
1986	Cook <i>et al.</i>	R-Band Cepheids	29.2	0.1
1992	Schmidt <i>et al.</i>	EPM - SN 1970G	29.34	+0.28 -0.49
1994	Pierce	<i>BRI</i> -Band T-F relation	29.2	0.5
1995	Alves & Cook	Cepheids & Mira stars	29.08	0.13
1996	Kelson <i>et al.</i>	HST Cepheids	29.34	0.17
1996	Feldmeier <i>et al.</i>	PNLF	29.42	0.15

TABLE 6

Distances to M51

Year	Author	Method and Data	$(m-M)_0$	σ
1974b	Sandage & Tammann	H II Regions	29.91	
1990	Georgiev <i>et al.</i>	Stellar Association Sizes	29.2	0.2
1994	Iwamoto <i>et al.</i>	SN 1994I - C+O stars	29.2	0.2
1996	Baron <i>et al.</i>	SN 1994I - SEAM	28.9	0.6
1996	Tonry	SBF	29.59	0.15
1996	This work	PNLF	29.62	0.15

TABLE 7

Distances to M96 (Including Leo Group)

Year	Author	Method and Data	$(m-M)_0$	σ
1977	Visvanathan & Sandage	Color-Magnitude relation	31.18	
1979	Visvanathan	Color-Magnitude relation	31.09	0.33
1982	de Vaucouleurs & Olson	Faber-Jackson relation	29.98	0.26
1983	Aaronson & Mould	Tully Fisher (on Leo Triplet)	29.84	0.25
1985	Pritchett & van den Bergh	Globular clusters LF	29.16	0.3
1988	Tonry & Schneider	Luminosity Fluctuations	29.96	
1989b	Ciardullo <i>et al.</i>	PNLF (group)	30.02	0.10
1990	Harris	Globular Clusters LF	30.19	0.43
1991	Tonry	Luminosity fluctuations (group)	29.84	
1995	Tanvir <i>et al.</i>	HST Cepheids	30.32	0.16
1996	Sakai <i>et al.</i>	Tip of RGB	30.20	0.14
1996	Graham <i>et al.</i>	HST Cepheids	30.01	0.19
1996	This work	PNLF	29.91	0.15

TABLE 8

Galaxies with PNLF and Cepheid Distances

Galaxy	Fitted Objects	Distance	Reference	Δ
M31	104 PNe	...	Ciardullo <i>et al.</i> 1989a	
	38 Cepheids	24.42 ± 0.10	Freedman & Madore 1990	...
LMC	58 PNe	$18.49^{+0.12}_{-0.14}$	Jacoby <i>et al.</i> 1990b	
	28 Cepheid	18.47 ± 0.10	Feast & Walker 1987	$+0.02^{+0.20}_{-0.21}$
NGC 300	25 PNe	$26.84^{+0.21}_{-0.29}$	Soffner <i>et al.</i> 1996	
	10 Cepheids	26.66 ± 0.10	Freedman <i>et al.</i> 1992	$+0.27^{+0.23}_{-0.31}$
M81	89 PNe	$27.78^{+0.08}_{-0.09}$	Jacoby <i>et al.</i> 1989	
	31 Cepheids	27.80 ± 0.17	Freedman <i>et al.</i> 1994	$-0.02^{+0.19}_{-0.19}$
NGC 5253 ^a	10 PNe	$28.14^{+0.14}_{-0.46}$	Phillips <i>et al.</i> 1992	
	12 Cepheids	27.94 ± 0.10	Saha <i>et al.</i> 1995	$+0.20^{+0.17}_{-0.47}$
M101	27 PNe	$29.42^{+0.09}_{-0.12}$	Feldmeier <i>et al.</i> 1996	
	29 Cepheids	29.34 ± 0.08	Kelson <i>et al.</i> 1996	$+0.08^{+0.12}_{-0.14}$
M96	33 PNe	$29.91^{+0.08}_{-0.10}$	This paper	
	7 Cepheids	30.32 ± 0.13	Tanvir <i>et al.</i> 1995	$-0.41^{+0.15}_{-0.16}$
	45 Cepheids	30.01 ± 0.16	Graham <i>et al.</i> 1996	$-0.10^{+0.18}_{-0.19}$

^aThe quoted distances to NGC 5253 assume a foreground galactic absorption of $A_B = 0.19$ from Burstein & Heiles (1984).

References

- Aaronson, M., & Mould, J. 1983, *Ap. J.*, **265**, 1
- Abell, G.O. 1975, *Exploration of the Universe*, (New York: Holt, Rinehart, & Wilson), p. 614
- Allen, C.W. 1973, *Astrophysical Quantities*, 3rd edition, (London: Athlone Press)
- Allen, R.J., Goss, W.M., & van Woerden, H. 1973, *Astr. Ap.*, **29**, 447
- Alves, D.R., & Cook, K.H. 1995, *A. J.*, **110**, 192
- Barbon, R., Cappellaro, E., & Turatto, M. 1989, *Astr. Ap. Suppl.*, **81**, 421
- Baron, E. 1996, private communication.
- Baron E., Hauschildt, P.H., Branch, D., Kirshner, R.P., & Filippenko, A.V. 1996, *M.N.R.A.S.*, **279**, 799
- Bottinelli, L., & Gouguenheim, L. 1976, *Astr. Ap.*, **51**, 275
- Bottinelli, L., Gouguenheim, L., Patrel, G., & de Vaucouleurs, G. 1984, *Astr. Ap. Suppl.*, **56**, 381
- Bottinelli, L., Gouguenheim, L., Patrel, G., & de Vaucouleurs, G. 1985, *Astr. Ap. Suppl.*, **59**, 43
- Bottinelli, L., Gouguenheim, L., Patrel, G., & Teerikorpi, P. 1991, *Astr. Ap.*, **252**, 550
- Bowen, I.S. 1951, *Carnegie Yrb.*, **50**, 17
- Burkhead, M.S. 1978, *Ap. J. Suppl.*, **38**, 147
- Burstein, D., & Heiles C. 1984, *Ap. J. Suppl.*, **54**, 33
- Buta, R., Corwin, H.G., de Vaucouleurs, G., de Vaucouleurs, A., & Longo, G. 1995, *A. J.*, **109**, 517
- Campbell, A. 1992, *Ap. J.*, **401**, 157
- Capaccioli, M., & Fasano, G. 1980, *Astr. Ap.*, **83**, 354
- Chevalier, R.A. 1982, *Ap. J.*, **251**, 259
- Chevalier, R.A. 1984, *Ann. N.Y. Acad. Sci.*, **422**, 215
- Ciardullo, R. 1995, *IAU Highlights of Astronomy*, 10, ed. I. Appenzeller (Dordrecht: Kluwer), p. 507
- Ciardullo, R., Ford, H.C., Neill, J.D., Jacoby, G.H., & Shafter, A.W. 1987, *Ap. J.*, **318**, 520
- Ciardullo, R., Jacoby, G.H., & Feldmeier J.J. 1997, *Ap. J.*, in preparation
- Ciardullo, R., Jacoby, G.H., & Ford, H.C. 1989b, *Ap. J.*, **344**, 715
- Ciardullo, R., Jacoby, G.H., Ford, H.C., & Neill, J.D. 1989a, *Ap. J.*, **339**, 53
- Ciardullo, R., Jacoby, G.H., & Harris, W.E. 1991, *Ap. J.*, **383**, 487

- Ciardullo, R., Jacoby, G.H., & Harris, W.E. 1996, *Ap. J.*, **462**, 1
- Ciardullo, R., Jacoby, G.H., & Tonry, J.L. 1993, *Ap. J.*, **419**, 479
- Cohen, J.G. 1993, *Bull. AAS*, **25**, 818
- Cook, K.H., Aaronson, M., & Illingworth, G. 1986, *Ap. J.*, **345**, 245
- de Vaucouleurs, G. 1958, *Ap. J.*, **128**, 465
- de Vaucouleurs, G. 1975, *Stars and Stellar Systems IX, Galaxies and the Universe*, ed. A. Sandage, M. Sandage, & J. Kristian (Chicago: University of Chicago Press), p. 557
- de Vaucouleurs, G. 1978, *Ap. J.*, **224**, 710
- de Vaucouleurs, G. 1979a, *Astr. Ap.*, **79**, 274
- de Vaucouleurs, G. 1979b, *Ap. J.*, **227**, 729
- de Vaucouleurs, G. 1993, *Ap. J.*, **415**, 10
- de Vaucouleurs, G., de Vaucouleurs, A., Corwin, H.G., Buta, R.J., Fouqué, P., & Paturel, G. 1991, *Third Reference Catalogue of Bright Galaxies*, (New York: Springer-Verlag)
- de Vaucouleurs, G., & Olson, D.W. 1982, *Ap. J.*, **256**, 346
- Disney, M.J., Davies, J.I., & Phillips, S. 1989, *M.N.R.A.S.*, **239**, 939
- Feast, M.W., & Walker, A.R. 1987, *Ann. Rev. Astr. Ap.*, **25**, 345
- Feldmeier, J.J., Ciardullo, R., & Jacoby, G.H. 1996, *Ap. J. (Letters)*, **461**, L25
- Ferrarese, L., Freedman, W.L., Hill, R.J., Saha, A., Madore, B.F., Kennicutt, R.C., Stetson, P.B., Ford, H.C., Graham, J.A., Hoessel, J.G., Han, M., Huchra, J., Hughes, S.M., Illingworth, G.D., Kelson, D., Mould, J.R., Phelps, R., Silbermann, N.A., Sakai, S., Turner, A., Harding, P., & Bresolin, F. 1996, *Ap. J.*, **464**, 568
- Fesen, R.A. 1993, *Ap. J. (Letters)*, **413**, L109
- Fesen, R.A., & Becker, R.H. 1990, *Ap. J.*, **351**, 437
- Freedman, W.L. 1996, in *Proceedings of the Space Telescope Science Institute Symposium on the Extragalactic Distance Scale*, in press
- Freedman, W.L., Hughes, S.M., Madore, B.F., Mould, J.R., Lee, M.G., Stetson, P., Kennicutt, R.C., Turner, A., Ferrarese, L., Ford, H., Graham, J.A., Hill, R., Hoessel, J.G., Huchra, J., & Illingworth, G.D. 1994, *Ap. J.*, **427**, 628

- Freedman, W.L., & Madore, B.F. 1990, *Ap. J.*, **365**, 186
- Freedman, W.L., Madore, B.F., Hawley, S.L., Horowitz, I.K., Mould, J., Navarrete, M., & Sallmen, S. 1992, *Ap. J.*, **396**, 80
- Geller, M.J., & Huchra, J.P. 1983, *Ap. J. Suppl.*, **52**, 61
- Georgiev, Ts.B., Getov, R.G., Zamanova, V.I., & Ivanov, G.R. 1990, *Pis. Astron. Zh.*, **16**, 979
- Giovanelli, R., Haynes, M.P., Salzer, J.J., Wegner, G., Da Costa, L.N., & Freudling, W. 1994, *A. J.*, **107**, 2036
- Gottesmann, S.T., Broderick, J.J., Brown, R.L., Balick, B., & Palmer, P. 1972, *Ap. J.*, **174**, 383
- Graham, J.A., Phelps, R.L., Freedman, W.L., Saha, A., Stetson, P.B., Madore, B.F., Silbermann, N.A., Sakai, S., Kennicutt, R.C., Harding, P., Turner, A., Mould, J.R., Ferrarese, L., Ford, H.C., Hoessel, J.G., Han, M., Huchra, J.P., Hughes, S.M., Illingworth, G.D., & Kelson, D.D. 1996, submitted to *ApJ*
- Han, Z., Podsiadlowski, P., & Eggleton, P.P. 1994, *M.N.R.A.S.*, **270**, 121
- Harris, W.E. 1990, *Pub. A.S.P.*, **102**, 966
- Holmberg, E. 1964, *Ark. f. Astr.*, **3**, 387
- Howard, S., & Byrd, G.G. 1990, *A. J.*, **99**, 1798
- Huchra, J.P., & Geller, M.J. 1982, *Ap. J.*, **257**, 423
- Hui, X., Ford, H.C., Ciardullo, R., & Jacoby, G.H. 1993, *Ap. J.*, **414**, 463
- Humason, M.L., Mayall, N.U., & Sandage, A. 1956, *A. J.*, **61**, 97
- Humphreys, R.M., & Aaronson, M. 1987, *Ap. J.*, **318**, L69
- Humphreys, R.M., Aaronson, M., Lebofsky, M., McAlary, C.W., Strom, S.E., & Capps, R.W. 1986, *A. J.*, **91**, 808
- Humphreys, R.M., & Strom, S.E. 1983, *Ap. J.*, **264**, 458
- Iwamoto, K., Nomoto, K., Hoflich, P., Yamaoka, H., Kumagai, S., & Shigeyama, T. 1994, *Ap. J. (Letters)*, **437**, 115
- Jaakkola, T., & Le Denmat, G. 1976, *M.N.R.A.S.*, **176**, 307
- Jacoby, G.H. 1989, *Ap. J.*, **339**, 39

- Jacoby, G.H., Branch, D., Ciardullo, R., Davies, R.L., Harris, W.E., Pierce, M.J., Pritchett, C.J.,
Tonry, J.L., & Welch, D.L. 1992, *Pub. A.S.P.*, **104**, 599
- Jacoby, G.H., Ciardullo, R., & Ford, H.C. 1990a, *Ap. J.*, **356**, 332
- Jacoby, G.H., Ciardullo, R., Ford, H.C., & Booth, J. 1989, *Ap. J.*, **344**, 70
- Jacoby, G.H., Ciardullo, R., & Harris, W.E. 1996, *Ap. J.*, **462**, 1
- Jacoby, G.H., Quigley, R.J., & Africano, J.L. 1987, *Pub. A.S.P.*, **99**, 672
- Jacoby, G.H., Walker, A.R., & Ciardullo, R. 1990b, *Ap. J.*, **365**, 471
- Kaler, J.B., & Jacoby, G.H. 1991, *Ap. J.*, **382**, 134
- Kelson, D.D., Illingworth, G.D., Freedman, W.L., Hill, R., Graham, J.A., Stetson, P.B., Saha, A.,
Madore, B.F., Kennicutt, R.C., Mould, J.R., Hughes, S.M., Ferrarese, L., Phelps, R., Turner,
A., Cook, K.H., Ford, H.C., Hoessel, J., & Huchra, J. 1996, *Ap. J.*, **463**, 26
- Kent, S.M. 1985, *Ap. J. Suppl.*, **59**, 115
- Lawrie, D.G., & Kwitter, K.B. 1982, *Ap. J.*, **255**, L29
- Leibundgut, B. 1994, in *Circumstellar Media in Late Stages of Stellar Evolution*, ed. R. Clegg, P.
Meikle, & I. Stevens (Cambridge: Cambridge Univ. Press), p. 100
- Long, K.S., Blair, W.P., & Krzeminski, W. 1989, *Ap. J. (Letters)*, **340**, L25
- Madore, B.F., & Freedman, W.L. 1991, *Pub. A.S.P.*, **103**, 933
- McClure, R.D., & Racine, R. 1969, *A. J.*, **74**, 1000
- McMillan, R., Ciardullo, R., & Jacoby, G.H. 1993, *Ap. J.*, **416**, 62
- Melnick, J. 1977, *Ap. J.*, **213**, 15
- Melnick, J., Heydari-Malayeri, M. & Leisy, P. 1992, *Astr. Ap.*, **253**, 16
- Méndez, R.H. 1996, in *I.A.U. Symposium 180, Planetary Nebulae*, ed. H. Habing & H. Lamers
(Dordrecht: Kluwer), in press
- Méndez, R.H., Kudritzki, R.P., Ciardullo, R., & Jacoby, G.H. 1993, *Astr. Ap.*, **275**, 534
- Pagal, B.E.J., Simonson, E.A., Terlevich, R.J., & Edmunds M.G. 1992, *M.N.R.A.S.*, **255**, 325
- Phillips, M.M., Jacoby, G.H., Walker, A.R., Tonry, J.L., & Ciardullo, R. 1992, *Bull. AAS*, **24**, 79
- Pierce, M.J. 1994, *Ap. J.*, **430**, 53
- Pritchett, C., & van den Bergh, S. 1985, *J.R.A.S.C.*, **79**, 240

- Renzini, A., & Buzzoni, A. 1986, in *Spectral Evolution of Galaxies*, ed. C. Chiosi, & A. Renzini (Dordrecht: Reidel), p. 195
- Richmond, M.W., Van Dyk, S.D., Ho, W., Peng, C., Paik, Y., Teffers, R.R., & Filippenko, A.V. 1996, *A. J.*, **111**, 327
- Rowan-Robinson, M. 1992, *M.N.R.A.S.*, **258**, 787
- Rozanski, R., & Rowan-Robinson, M. 1994, *M.N.R.A.S.*, **271**, 530
- Rupen, M.P., Sramek, R.A., Van Dyk, S.D., Weiler, K.W., & Panagia, N. 1994, *IAU Circ.* No. 5963
- Saha, A., Sandage, A., Labhardt, L., Schwengeler, H., Tammann, G.A., Panagia, N., & Macchetto, F.D. 1995, *Ap. J.*, **438**, 8
- Saha, A., Sandage, A., Labhardt, L., Tammann, G.A., Macchetto, F.D., & Panagia, N. 1996, *Ap. J.*, in press.
- Sakai, S., Madore, B.F., Freedman, W.L., Lauer, T.R., Ajhar, E.A., & Baum, W.A. 1996, *Ap. J.*, in press.
- Sandage, A. 1983, *A. J.*, **88**, 1569
- Sandage, A., & Tammann, G.A. 1974a, *Ap. J.*, **194**, 223
- Sandage, A., & Tammann, G.A. 1974b, *Ap. J.*, **194**, 559
- Sandage, A., & Tammann, G.A. 1976, *Ap. J.*, **210**, 7
- Sandage, A., & Tammann, G.A. 1987, *A Revised Shapley-Ames Catalog of Bright Galaxies*, (Washington: Carnegie Institution of Washington)
- Schmidt, B.P., Kirshner, R.P., & Eastman, R.G. 1992, *Ap. J.*, **395**, 366
- Schneider, S.E. 1989, *Ap. J.*, **343**, 94
- Schneider, S.E., Skrutskie, M.F., Hacking, P.B., Young, J.S., & Dickman, R.L. 1989, *A. J.*, **97**, 666
- Schönberner, D. 1981, *Astr. Ap.*, **103**, 119
- Schönberner, D. 1983, *Ap. J.*, **272**, 708
- Shaver, P.A., McGee, R.X., Newton, L.M., Danks, A.C., & Pottasch S.R. 1983, *M.N.R.A.S.*, **204**, 53
- Seaton, M.J. 1979, *M.N.R.A.S.*, **187**, 73p

- Silbermann, N.A., Harding, P., Madore, B.F., Kennicutt, R.C., Saha, A., Stetson, P.B., Freedman, W.L., Mould, J.R., Graham, J.A., Hill, R.J., Turner, A., Bresolin, F., Ferrarese, L., Ford, H., Hoessel, J.G., Han, M., Hughes, S.M.G., Illingworth, G.D., Phelps, R., & Sakai, S. 1996, *Ap. J.*, in press.
- Soffner, T., Méndez, R.H., Jacoby, G.H., Ciardullo, R., Roth, M.M., & Kudritzki, R.P. 1996, *Astr. Ap.*, **306**, 9
- Stanghellini, L. 1995, *Ap. J.*, **452**, 515
- Stetson, P.B. 1987, *Pub. A.S.P.*, **99**, 191
- Stone, R.P.S. 1977, *Ap. J.*, **218**, 767
- Storchi-Bergmann, T., Calzetti, D., & Kinney, A.L. 1994, *Ap. J.*, **429**, 572
- Tanvir, N.R., Shanks, T., Ferguson, H.C., & Robinson, D.R.T. 1995, *Nature*, **377**, 27
- Tonry, J.L. 1991, *Ap. J. (Letters)*, **373**, L1
- Tonry, J.L. 1996, private communication
- Tonry, J.L., Ajhar, E.A., & Luppino, G.A. 1990, *A. J.*, **100**, 1416
- Tonry, J.L., & Schneider, D.P. 1988, *A. J.*, **96**, 807
- Toomre, A., & Toomre, J. 1972, *Ap. J.*, **178**, 623
- Tully, R.B. 1988, *Nearby Galaxies Catalog*, (Cambridge: Cambridge University Press)
- Turner, E.L., & Gott, J.R. 1976, *Ap. J. Suppl.*, **32**, 409
- Valentijn, E.A. 1990, *Nature*, **346**, 153
- Vennik, J. 1984, *Tartu Astr. Obs., Teated*, 73, 3
- Visvanathan, N. 1979, *Ast. Soc. Aus. Proc.*, **3**, 309
- Visvanathan, N., & Sandage, A. 1977, *Ap. J.*, **216**, 214
- Walsh, J.R., & Roy, J.R. 1989, *M.N.R.A.S.*, **239**, 297
- Wray, J.D., & de Vaucouleurs, G. 1980, *A. J.*, **85**, 1
- Welch, D.L., McAlary, C.W., McLaren, R.A., & Madore, B.F. 1986, *Ap. J.*, **305**, 583

Figure Captions

Figure 1: The planetary nebula luminosity functions for M101, M51, and M96 binned into 0.2 mag, 0.2 mag, and 0.15 mag intervals respectively. The solid lines represent the empirical PNLF of equation (1) convolved with the mean photometric error vs. magnitude relation and translated to the most likely distance modulus for each galaxy. The solid circles represent objects in our statistical PN samples; the open circles indicate objects fainter than the completeness limit that were not included in the maximum likelihood solution.

Figure 2: An [O III] $\lambda 5007$ image of M51, with the positions of our PN candidates marked by plus signs. North is up, and east is to the left; the image is $16'$ on a side. Note the large number of planetary nebulae to the west of NGC 5195. This region corresponds to the increase in surface brightness seen in the deep images of Burkhead (1978).

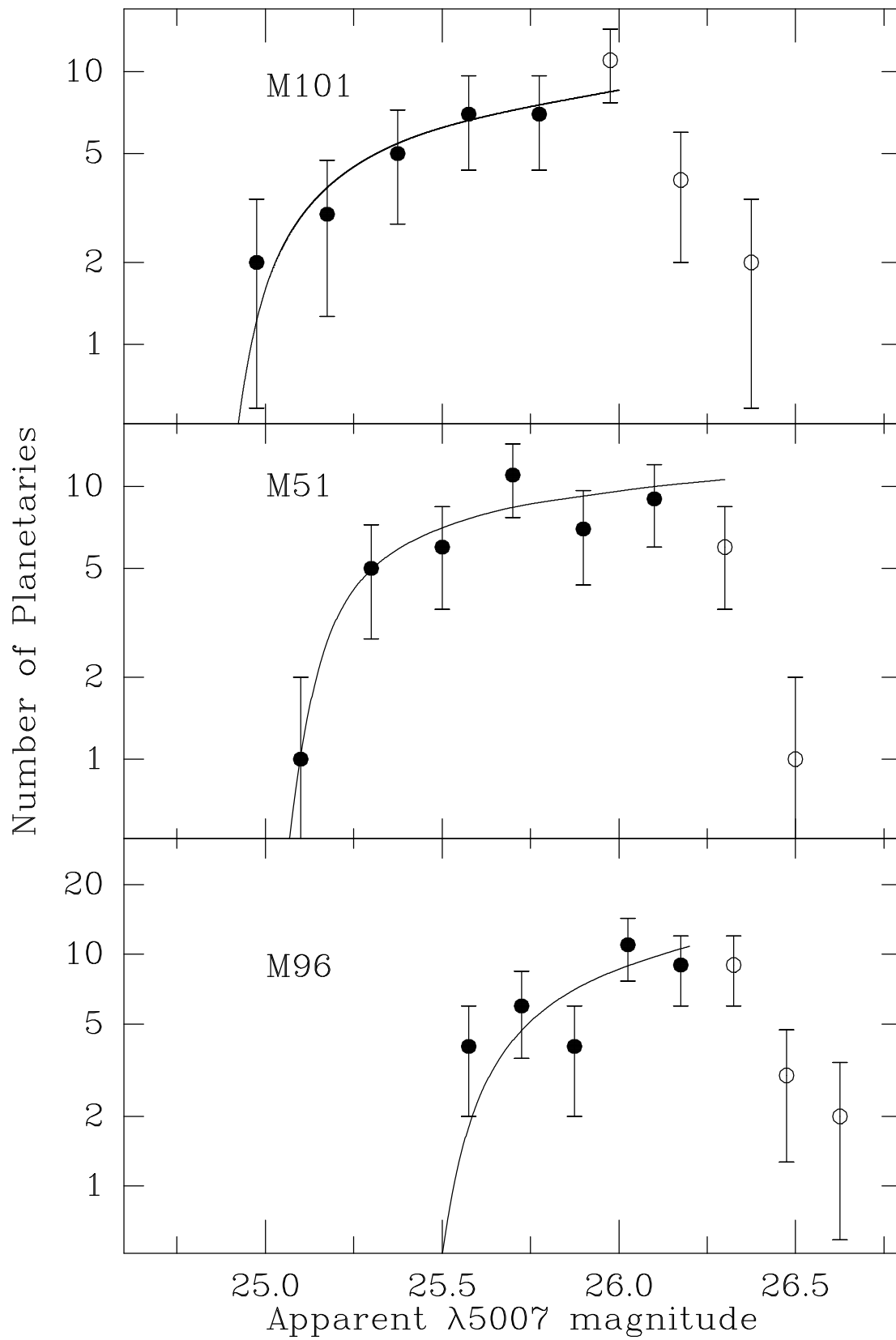
Figure 3: An [O III] $\lambda 5007$ image of M96, with the positions of our PN candidates marked by plus signs. North is up, and east is to the left; the image is $16'$ on a side. Again, the planetaries are found most easily in the outskirts of the galaxy.

Figure 4: The effect of internal extinction on our derived distance to M101, assuming the scale height of dust and PN in the galaxy is the same as that in Milky Way. The abscissa represents the total amount of extinction at 5007 \AA perpendicular to the galactic plane. Note that no matter how much extinction is present in M101, the derived PNLF distance never varies by more than 0.1 mag from the case of no internal extinction.

Figure 5: Images of the region around SN 1970G. The on-band image is on the left, the off-band image is on the right. North is up, and east is to the left; the regions displayed are $23''.5$ on a side. The $2''.35$ radius circles are centered around the estimated position of the supernova. The supernova is present in the off-band, but is invisible on the on-band frame.

Figure 6: Images of the region around SN 1951H. The on-band image is on the left; the off-band image is on the right. North is up, and east is to the left; the regions shown are $47''$ on a side. The plus signs in the center of the images are at the position of the supernova, as given by Barbon, Cappellaro, & Turatto (1989). The plus sign to the left and slightly above the image centers, are our best estimate of the supernova position from visual inspection of an historical image.

Figure 7: A plot showing the distances to galaxies with both PNLF and Cepheid distance determinations. Filled circles represent direct comparisons between galaxies. Open circles show comparisons of different galaxies within the same cluster, and have arbitrary 1 Mpc error bars. Note the extremely good agreement over two orders of magnitude. With the exception of M96, the scatter about the residuals is entirely consistent with the errors.

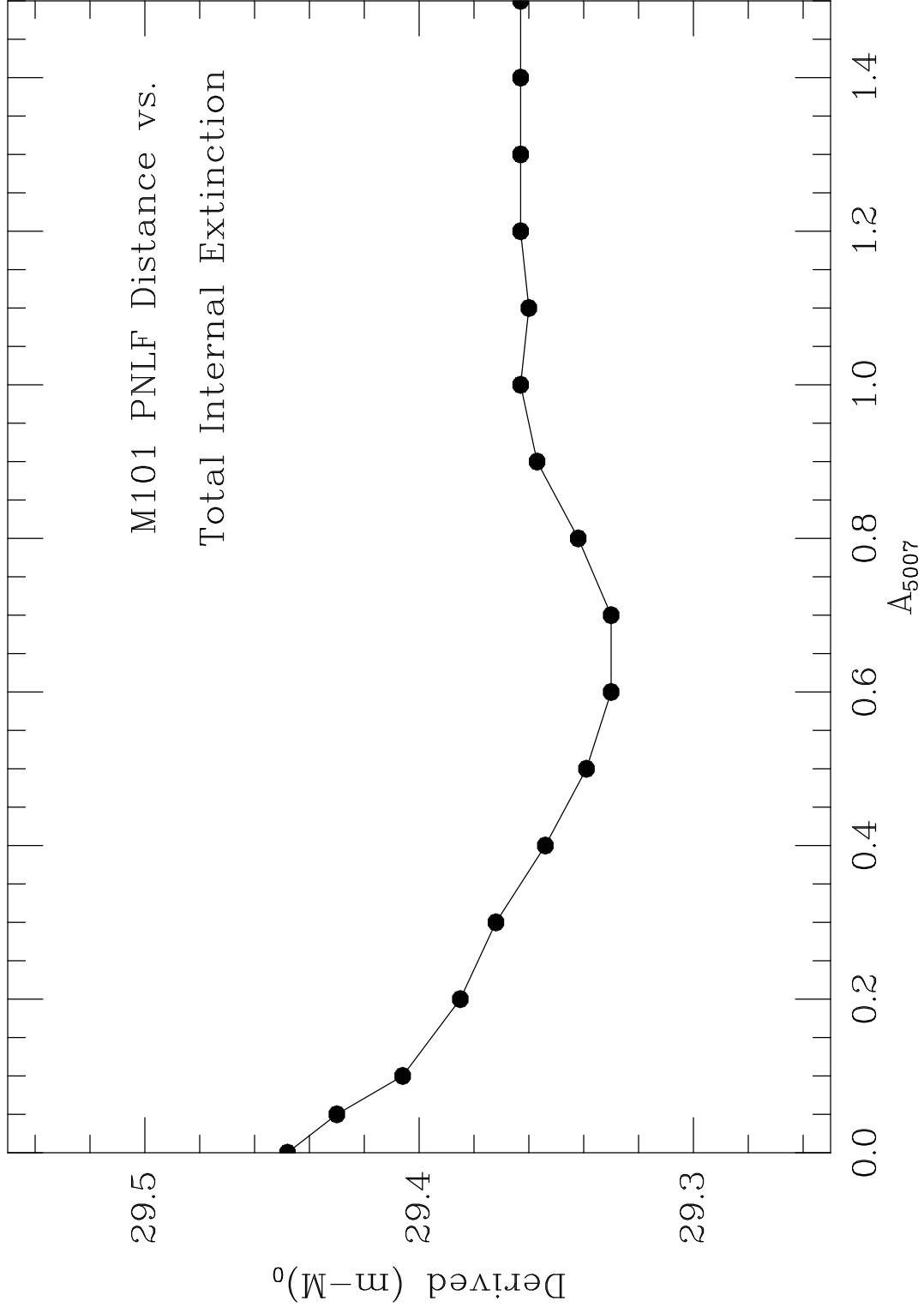


This figure "spirals_fig2.jpg" is available in "jpg" format from:

<http://arxiv.org/ps/astro-ph/9611041v1>

This figure "spirals_fig3.jpg" is available in "jpg" format from:

<http://arxiv.org/ps/astro-ph/9611041v1>



This figure "spirals_fig5.gif" is available in "gif" format from:

<http://arxiv.org/ps/astro-ph/9611041v1>

This figure "spirals_fig6.jpg" is available in "jpg" format from:

<http://arxiv.org/ps/astro-ph/9611041v1>

